PHYSICAL REVIEW A
GENERAL PHYSICS

THIRD SERIES, VOLUME 40, NUMBER 5 SEPTEMBER 1, 1989

Relativistic all-order calculations of energies and matrix elements for Li and Be$^+$

S. A. Blundell, W. R. Johnson, Z. W. Liu, and J. Sapirstein
University of Notre Dame, Notre Dame, Indiana 46556

(Received 13 April 1989)

Valence removal energies, hyperfine constants, and *E*1 transition amplitudes are calculated for the $2s_{1/2}$, $2p_{1/2}$, $2p_{3/2}$, and $3s_{1/2}$ states of Li and Be$^+$. This calculation is an extension of earlier second- and third-order many-body perturbation theory (MBPT) calculations, in which now an infinite subset of MBPT terms is evaluated using all-order methods. Agreement with experiment at the 0.01% level for energies, and at the 0.1% level for matrix elements, is found. Issues involved with those higher-order terms omitted by the technique are discussed.

I. INTRODUCTION

Despite the well-understood nature of electromagnetism, the force that binds atoms, highly accurate calculations of the properties of atoms with more than two electrons are difficult and relatively rare. Recently, however, Lindgren[1] has presented a nonrelativistic (NR) coupled-cluster calculation of the energy levels and hyperfine constants of neutral lithium in which he sums infinite sets of many-body perturbation theory (MBPT) terms and obtains very close agreement with experiment—on the order of 0.01% for energies and under 1% for matrix elements. We have found good, but less precise, agreement in a set of calculations that (while relativistic) are limited to second order for energies and to third order for matrix elements.[2] Specifically, energy levels differ from experiment on the order of 0.1%, while matrix elements differed by under 1% with the exception of the hyperfine constant of the $2p_{3/2}$ state, which differed from experiment by 18%. By including third-order corrections we were able to improve the agreement with experiment for energies to the level of 0.05% for Li and Be$^+$.[3] It is the purpose of the present paper to report the results of relativistic all-order calculations that add to our previous work the relativistic generalization of the higher-order terms considered by Lindgren.[1] We obtain energies in the same very precise agreement with experiment as in Ref. 1, and matrix elements in agreement with experiment at the 0.1% level. The techniques used for neutral lithium are also applicable to other members of the lithium isoelectronic sequence. We extend our calculations to the first ion of this sequence, Be$^+$, and find similar agreement with experiment. While the accuracy achieved in this work is high by the standards of MBPT, it should be noted that NR variational techniques have recently been applied to the ground states of Li and Be$^+$ by King and Shoup[4] with even higher accuracy.

There is considerable flexibility in the choice of all-order methods. For this reason we explicitly describe the scheme used in this work in Sec. II. Numerical results are given in Sec. III, along with a comparison with experiment. Finally, in Sec. IV, we discuss the terms in higher orders of MBPT that are left out of our all-order method, and the prospects for accounting for such omitted terms. A technical discussion of the treatment of disconnected terms is given in the Appendix.

II. ALL-ORDER FORMULAS FOR ENERGIES AND MATRIX ELEMENTS

A. Energies

Lithiumlike ions consist of a valence electron outside a filled heliumlike core. We have recently employed relativistic all-order methods to describe helium.[5] We briefly reprise the results from that work and describe the extensions required for a description of one-valence-electron systems. This leads to a derivation of all-order equations for three-electron systems essentially equivalent to the configuration-interaction[6] (CI) approach, in which the Hamiltonian is diagonalized within a subspace of the many-electron Hilbert space. We shall present this derivation first in some detail, and then briefly outline an alternative derivation within the framework of the coupled-cluster approach.

The exact two-particle wave function can be obtained from the lowest-order Hartree-Fock (HF) wave function, $|0_C\rangle$, as

$$|\Psi\rangle=\left[1+\sum_{ma}\rho_{ma}a_m^\dagger a_a+\frac{1}{2}\sum_{mnab}\rho_{mnab}a_m^\dagger a_n^\dagger a_b a_a\right]|0_C\rangle . \quad (1)$$

Here we are using intermediate normalization; to normalize the wave function one must multiply by $N_C^{-1/2}$, where

$$N_C=1+\sum_{ma}\rho_{ma}^*\rho_{ma}+\frac{1}{2}\sum_{mnab}\rho_{mnab}^*\tilde{\rho}_{mnab} , \quad (2)$$

with $\tilde{\rho}_{ijkl}\equiv\rho_{ijkl}-\rho_{ijlk}$. In Eqs. (1) and (2), sums over *a* and b run over the occupied core and sums over m and n run over all positive-energy states outside the core; all single-particle states here are defined in the HF potential. Negative-energy states are specifically omitted from the excited-state summations; they are connected with QED effects that are negligible at the level of accuracy of this work. Substituting Eq. (1) into $H|\Psi\rangle = E|\Psi\rangle$, we find

$$(\varepsilon_a + \delta E_C - \varepsilon_m)\rho_{ma} = \sum_{bn} \tilde{g}_{mban}\rho_{nb} + \sum_{bnr} g_{mbnr}\tilde{\rho}_{nrab} - \sum_{bcn} g_{bcan}\tilde{\rho}_{mnbc} , \tag{3a}$$

$$\begin{aligned}(\varepsilon_a + \varepsilon_b + \delta E_C - \varepsilon_m - \varepsilon_n)\rho_{mnab} &= g_{mnab} + \sum_{cd} g_{cdab}\rho_{mncd} + \sum_{rs} g_{mnrs}\rho_{rsab} \\ &\quad + \left[\sum_r g_{mnrb}\rho_{ra} - \sum_c g_{cnab}\rho_{mc} + \sum_{cr} \tilde{g}_{cnrb}\tilde{\rho}_{mrac}\right] \\ &\quad + \begin{bmatrix} a \leftrightarrow b \\ m \leftrightarrow n \end{bmatrix} ,\end{aligned} \tag{3b}$$

$$\begin{aligned} E &= E_{\mathrm{HF}} + \delta E_C , \\ E_{\mathrm{HF}} &= \sum_a \varepsilon_a - \tfrac{1}{2}\sum_{ab} \tilde{g}_{abab} , \\ \delta E_C &= \tfrac{1}{2} \sum_{abmn} g_{abmn}\tilde{\rho}_{mnab} . \end{aligned} \tag{3c}$$

Here g_{ijkl} is the Coulomb matrix element,

$$g_{ijkl} \equiv \int \frac{d^3r\, d^3r'}{|\mathbf{r}-\mathbf{r}'|} \psi_i^\dagger(\mathbf{r})\psi_k(\mathbf{r})\psi_j^\dagger(\mathbf{r}')\psi_l(\mathbf{r}') . \tag{4}$$

To generalize the above equations to the lithium case, we write the lowest-order state as

$$|0_v\rangle \equiv a_v^\dagger|0_C\rangle , \tag{5}$$

where the single-particle states are defined in the HF potential of the heliumlike core, and $|0_C\rangle$ is the HF wave function for this core. This state can be modified in three ways. First, the core can be modified exactly as in Eq. (1); second, a modification in which one of the core states is replaced by the valence state can be made. We will include these two modifications in the following, and write

$$\begin{aligned}|\Psi_v\rangle = \Bigg[1 &+ \sum_{ma} \rho_{ma} a_m^\dagger a_a + \tfrac{1}{2} \sum_{mnab} \rho_{mnab} a_m^\dagger a_n^\dagger a_b a_a \\ &+ \sum_{m\neq v} \rho_{mv} a_m^\dagger a_v + \sum_{mna} \rho_{mnva} a_m^\dagger a_n^\dagger a_a a_v \Bigg]|0_v\rangle .\end{aligned} \tag{6}$$

To normalize this wave function, we must multiply by $N_v^{-1/2}$, where

$$\begin{aligned}N_v = N_C &+ \sum_m \rho_{mv}^*\rho_{mv} - \sum_a \rho_{va}^*\rho_{va} + \sum_{abm} \rho_{vmab}^*\tilde{\rho}_{mvab} \\ &+ \sum_{mna} \rho_{mnva}^*\tilde{\rho}_{mnva} + \sum_{ma} (\tilde{\rho}_{vmva}\rho_{ma}^* + \tilde{\rho}^{\,*}_{vmva}\rho_{ma}) .\end{aligned} \tag{7}$$

The third possible modification, which we will not consider in this paper, is to destroy both electrons in the core and also the valence electron. The corresponding correction to the wave function would be described by

$$|\delta\psi_v\rangle = \sum_{mnrab} \rho_{mnrvab} a_m^\dagger a_n^\dagger a_r^\dagger a_a a_b a_v |0_v\rangle . \tag{8}$$

We are forced to neglect such a term because of the difficulty of dealing with ρ_{mnrvab}. In order to carry out multiple summations over excited states with the accuracy of interest, we require large basis sets and a large number of angular momentum channels. The size of the basis sets makes the treatment of even the simpler object ρ_{mnab} difficult. The resulting numerical computations require the use of supercomputers, so inclusion of Eq. (8) is not practical at present. We believe, however, that such effects can be treated adequately using perturbation theory; the excellent agreement with experiment shown in Sec. III is empirical evidence for this belief.

We now apply Schrödinger's equation to the approximate wave function (6). The action of the potential on the wave function results in terms involving one, three, five, seven, and nine creation or destruction operators acting on the core $|0_C\rangle$. The terms with nine operators vanish for three-electron systems since they involve four destruction operators. Terms with seven operators would have to be considered if the wave function correction of Eq. (8) were included, but since we are not including this correction, we drop such terms. As a further approximation we drop those terms having seven operators with both a valence creation operator and a valence destruction operator, even though by using the anticommutation relations these could be reduced to terms with five operators. Because of this approximation, our formalism omits certain terms in third-order MBPT, which are included in other formalisms.[7] We discuss this approximation further below. After these approximations, we are in a position to identify the coefficients of the three and five operator terms, and find

$$[\varepsilon_a - \varepsilon_m + (\delta E_C + \delta E_v)]\rho_{ma} = \sum_{bn} \tilde{g}_{mban}\rho_{nb} + \sum_{bnr} g_{mbnr}\tilde{\rho}_{nrab} - \sum_{bcn} g_{bcan}\tilde{\rho}_{mnbc} , \tag{9a}$$

$$\begin{aligned}[\varepsilon_a + \varepsilon_b - \varepsilon_m - \varepsilon_n + (\delta E_C + \delta E_v)]\rho_{mnab} &= g_{mnab} + \sum_{cd} g_{cdab}\rho_{mncd} + \sum_{rs} g_{mnrs}\rho_{rsab} \\ &\quad + \left[\sum_r g_{mnrb}\rho_{ra} - \sum_c g_{cnab}\rho_{mc} + \sum_{cr} \tilde{g}_{cnrb}\tilde{\rho}_{mrac}\right] \\ &\quad + \begin{bmatrix} a \leftrightarrow b \\ m \leftrightarrow n \end{bmatrix} ,\end{aligned} \tag{9b}$$

$$\begin{aligned}[\varepsilon_v - \varepsilon_m + (\delta E_C) + \delta E_v]\rho_{mv} &= \sum_{an} \tilde{g}_{mavn}\rho_{na} + \sum_{anr} g_{manr}\tilde{\rho}_{nrva} \\ &\quad - \sum_{abr} g_{abvr}\tilde{\rho}_{mrab} ,\end{aligned} \tag{9c}$$

$$\begin{aligned}[\varepsilon_a + \varepsilon_v - \varepsilon_m - \varepsilon_n + (\delta E_C) + \delta E_v]\rho_{mnva} &= g_{mnva} + \sum_{bc} g_{bcva}\rho_{mnbc} + \sum_{rs} g_{mnrs}\rho_{rsva} \\ &\quad + \left[\sum_r g_{mnra}\rho_{rv} - \sum_b g_{bnva}\rho_{mb} + \sum_{br} \tilde{g}_{bnra}\tilde{\rho}_{mrvb}\right] \\ &\quad + \begin{bmatrix} a \leftrightarrow v \\ m \leftrightarrow n \end{bmatrix} ,\end{aligned} \tag{9d}$$

$$E = E_{\mathrm{HF}} + \delta E_C + \varepsilon_v + \delta E_v ,$$

where E_{HF} and δE_C are given by Eq. (3c), and where

$$\delta E_v = \sum_{ma} \tilde{g}_{vavm}\rho_{ma} + \sum_{mab} g_{abvm}\tilde{\rho}_{mvab} + \sum_{mna} g_{vamn}\tilde{\rho}_{mnva} \ . \tag{10}$$

As $E_{\mathrm{HF}}+\delta E_C$ corresponds physically to the energy of the ion core, $\varepsilon_v+\delta E_v$ may be identified as the negative of the valence ionization energy. The Goldstone diagrams for δE_v are drawn in Fig. 1. The final approximation that we make is to neglect the energy shifts given in small parentheses in Eqs. (9a)–9(d). Without these energy shifts, our equations are equivalent to a simplified version of the coupled-cluster approach in the pair approximation.

The coupled-cluster (CC) formalism[1,8] enables one to construct all-order equations whose iteration leads to a term-by-term identification with the Rayleigh-Schrödinger linked-diagram expansion. The formalism thus shares with the order-by-order approach the property of being size consistent, which could be important for accurate calculations on heavy elements. In addition, use of the CC approach enables one to combine the all-order technique with MBPT. It is possible to identify unambiguously which MBPT diagrams have been included implicitly in any CC scheme and which have been omitted. The most important omitted diagrams can then be added using low-order MBPT.

As shown by Lindgren and Morrison,[9] for example, it is possible to write the exact many-body wave function (in intermediate normalization) as

$$|\psi_v\rangle = \{\exp(S)\}|0_v\rangle \ , \tag{11}$$

where S is an operator which can be represented by connected Goldstone diagrams, and $|0_v\rangle$ is the zeroth-order wave function, in our case given by Eq. (5). Operators inside the braces $\{\ldots\}$ are to be normally ordered with respect to the core, that is, rearranged such that core creation and excited annihilation operators lie to the right of core annihilation and excited creation operators, with the insertion of an appropriate phase. For an N-body system, S may be decomposed into contributions in which one, two, three, etc., N electrons are excited from $|0_v\rangle$

$$S = S_1 + S_2 + \cdots + S_N \ . \tag{12}$$

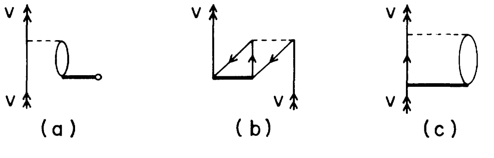

FIG. 1. Brueckner-Goldstone graphs representing the valence energy in Eq. (10). Dashed lines represent Coulomb matrix elements g_{mnab}, solid lines ending in a circle represent the one-particle excitation operator ρ_{ma}, and solid lines represent the two-particle excitation operator ρ_{mnab}. Exchange graphs are not explicitly shown.

For three-electron systems,

$$\begin{aligned}|\psi_v\rangle &= \{\exp(S_1+S_2+S_3)\}|0_v\rangle \\ &= \{(1+S_1+S_2+S_3+\tfrac{1}{2}S_2^2+S_1S_2+\cdots)\}|0_v\rangle \ .\end{aligned} \tag{13}$$

Our all-order equations are equivalent to neglecting the triple excitation terms S_3 and all nonlinear terms,

$$|\psi_v\rangle = \{(1+S_1+S_2)\}|0_v\rangle \ . \tag{14}$$

We shall refer to the omitted nonlinear terms as *coupled-cluster* terms; the most important are $\frac{1}{2}S_2^2$ and S_1S_2. After these approximations, one can follow the method outlined by, for example, Lindgren and Morrison[9] to obtain the all-order Eqs. (9a)–9(d) with the energy shifts in small parentheses absent. When the equations are iterated, these energy shifts would lead to terms not present in the linked-diagram expansion for a general atom. Furthermore, these terms can be shown to destroy the size consistency of the approximation. Note, however, that the valence correlation energy is retained in the energy factor for the valence Eqs. (9c) and (9d); this term is associated with *folded* diagrams.

The neglected coupled-cluster terms can be shown to lead to energy and matrix element corrections starting in fourth order. The neglect of S_3, however, leads to errors already in third order for valence ionization energies. We have identified the omitted third-order terms, and include them as a correction $E^{(3)}_{\mathrm{extra}}$; explicit expressions for these terms are given in Ref. 3. As shown by Lindgren,[7] these omitted third-order terms are, in fact, of a type which can be picked up in the pair approximation by the use of a Hermitian reformulation of the CC approach. (Also, they are the contributions mentioned above in the CI derivation that arise from the neglect of terms with seven annihilation and creation operators acting on $|0_C\rangle$.) However, as $E^{(3)}_{\mathrm{extra}}$ is already a small correction, we shall not investigate this Hermitian formulation at the present stage. With the addition of $E^{(3)}_{\mathrm{extra}}$, our equations are complete through third-order MBPT; the principal omitted terms are the fourth-order coupled-cluster terms, and the fourth-order triples.

It should be noted that, for three-electron systems, it is in fact possible to pick up a valid subset of CC terms by including δE_C in the energy factor in Eq. (9a) and (9b). It is possible to show that such a term in (9a) corresponds exactly to the inclusion of S_1S_2 in (14), while in (9b) it corresponds to the inclusion of $\frac{1}{2}S_2^2$ in (14), when there are two electrons in the core. Furthermore, as may be seen from (3a)–3(c), this modification causes the two-electron core energy to be given exactly by the all-order formalism. We have nevertheless chosen not to include this term in the present calculation for two main reasons. Firstly, because we are primarily interested in valence properties in the present work, and the modification mentioned leads only to a subset of the fourth-order CC corrections to valence removal energies or matrix elements. There are, in addition, fourth-order CC terms associated with the valence equations (9c) and (9d) that can-not be included merely through energy shifts, while for matrix elements the formula (21) must be augmented with extra terms. The second reason is that this simplicity is special to systems with two-electron cores; for larger atoms, such a modification of (9a) and (9b) does not lead to an exact core energy, and in fact introduces spurious terms, as discussed below Eq. (14). It is our hope to extend the present treatment to the whole series of alkali-metal atoms, with the present calculation the first in the series.

In addition to the above all-order treatment of the Coulomb correlation, we employ MBPT to add terms arising from the Breit interaction and from nuclear recoil. These contributions have been evaluated as described for Na-like ions in Ref. 10, and differ from our previously reported results for Li-like systems[3] by the addition of higher-order terms, and by the explicit evaluation of the mass-polarization effect rather than use of the Hughes-Eckart formula.[11] Specifically, for the Breit interaction, we include the lowest-order term, plus a random-phase approximation- (RPA)-like summation of the one-body part of the Breit interaction, plus residual second-order corrections and a third-order correction associated with Brueckner orbitals. For nuclear recoil, we add the reduced-mass contribution $(m_e/M_{\mathrm{nuc}})\varepsilon_v$ and treat correlation corrections to the mass polarization as described above for the Breit interaction. As explained in Ref. 10, we are here using a nonrelativistic approximation for nuclear recoil (except that the expectation value of the nonrelativistic mass-polarization operator is taken with relativistic wave functions). This approximation is adequate, for the nuclear recoil correction (Table II) is already small, and relativistic corrections to it are expected to be suppressed by a further factor of α^2 in neutral or nearly neutral atoms, putting them well below the level of significance of the present calculation. In general, a fully consistent relativistic formulation of nuclear recoil in many-electron atoms remains an outstanding problem.

B. Matrix elements

We now turn to a discussion of the evaluation of the matrix element of a one-body operator Z,

$$M_{wv}=\frac{\langle\psi_w|Z|\psi_v\rangle}{\sqrt{\langle\psi_w|\psi_w\rangle\langle\psi_v|\psi_v\rangle}}\ , \tag{15}$$

with

$$Z=\sum_{i=1}^{N} z_i$$

between states having a single valence electron outside closed shells. It is useful to separate the numerator of this expression into a zero-body (or core) contribution, and a one-body (or valence) contribution, as follows. Writing

$$|\psi_v\rangle=\Omega_v a_v^\dagger|0_C\rangle\ , \tag{16}$$

we have

$$\langle\psi_w|Z|\psi_v\rangle=\langle 0_C|a_w(\Omega_w^\dagger Z\Omega_v)a_v^\dagger|0_C\rangle=Z_0+Z_1\ ,$$

where

$$Z_0=\delta_{wv}\langle 0_C|\Omega_w^\dagger Z\Omega_v|0_C\rangle$$

and

$$Z_1=\langle 0_C|\overline{a_w(\Omega_w^\dagger Z\Omega_v)a_v^\dagger}|0_C\rangle\ . \tag{17}$$

The zero-body term Z_0 is formed after contraction of a_w and $a_v^\dagger$, and is nonzero only for diagonal matrix elements $(v=w)$. The remaining terms Z_1 are ones in which a_w and $a_v^\dagger$ contract into $\Omega_w^\dagger Z\Omega_v$; this is the meaning of the bar notation. It is also useful to make a similar distinction with the normalized terms

$$\begin{aligned}&\langle\psi_v|\psi_v\rangle=N_0+\delta N_v\ ,\\&N_0=\langle 0_C|\Omega_v^\dagger\Omega_v|0_C\rangle\ ,\\&\delta N_v=\langle 0_C|\overline{a_v(\Omega_v^\dagger\Omega_v)a_v^\dagger}|0_C\rangle\ .\end{aligned} \tag{18}$$

The core normalization N_0 is in fact independent of v, as terms in Ω_v which depend on v give vanishing contributions.

A direct way to evaluate M_{wv} in the pair approximation is to substitute Eq. (6) for the wave function into the numerator and denominator of Eq. (15). However, inspection of the various terms that result reveals disconnected terms, showing that this formulation is not size consistent. Specifically, terms appear on the numerator having the form of matrix elements of Z multiplied by the core normalization; such terms cancel against only the leading order of a binomial expansion of the denominator, leaving higher-order disconnected terms.

These disconnected contributions in fact vanish in a complete treatment, as is shown by the following identity which holds for exact wave functions:

$$M_{wv}=\delta_{wv}(Z_0)_{\mathrm{conn}}+\frac{(Z_1)_{\mathrm{conn}}}{\{[1+(\delta N_w)_{\mathrm{conn}}][1+(\delta N_v)_{\mathrm{conn}}]\}^{1/2}}\ . \tag{19}$$

This result is proved in the Appendix. The subscript "conn" indicates that terms represented by disconnected Goldstone diagrams are to be discarded; the contributions must be rigorously connected. This identity is just the generalization to one-valence-electron systems of the well-known result for closed-shell systems,[12]

$$\frac{\langle\psi|Z|\psi\rangle}{\langle\psi|\psi\rangle}=\langle\psi|Z|\psi\rangle_{\mathrm{conn}}\ . \tag{20}$$

Notice, however, that for one-valence-electron systems there is a residual normalization contribution to the one-body part of the matrix element associated with the connected terms from δN_v and δN_w. We shall refer to $(\delta N_v)_{\mathrm{conn}}$ as the valence normalization in the following. If the denominator is expanded using the binomial theorem, one obtains the *folded* contributions to the matrix element.

A size-consistent formulation of the matrix element can now be achieved by substituting the approximate wave functions Eq. (6) into Eq. (19) rather than into Eq. (15). The core part Z_0 vanishes if the operator Z is nonscalar, as is the case for all properties considered here; we shall not consider this term any further. By use of Wick's theorem, we find that $(Z_1)_{\rm conn}$ consists of the lowest-order result z_{wv} corrected by the set of 20 terms shown in Fig. 2. The analytical expressions are

$$(Z_1)_{\rm conn} = z_{wv} + Z_{wv}^{(a)} + Z_{wv}^{(b)} + \cdots + Z_{wv}^{(t)} \,, \tag{21}$$

where

$$\begin{aligned}
Z_{wv}^{(a)} &= \sum_{am} z_{am} \widetilde{\rho}_{wmva} + \text{c.c.} \,, \\
Z_{wv}^{(b)} &= -\sum_{a} z_{av} \rho_{wa} + \text{c.c.} \,, \\
Z_{wv}^{(c)} &= \sum_{m} z_{wm} \rho_{mv} + \text{c.c.} \,, \\
Z_{wv}^{(d)} &= \sum_{mn} \rho^{*}_{nw} z_{nm} \rho_{mv} \,, \\
Z_{wv}^{(e)} &= \sum_{ab} \rho^{*}_{vb} z_{ab} \rho_{wa} \,, \\
Z_{wv}^{(f)} &= -\sum_{am} \rho^{*}_{mw} z_{av} \rho_{ma} + \text{c.c.} \,, \\
Z_{wv}^{(g)} &= -\sum_{am} \rho^{*}_{ma} z_{mv} \rho_{wa} + \text{c.c.} \,, \\
Z_{wv}^{(h)} &= \sum_{mna} \rho^{*}_{mw} z_{an} \widetilde{\rho}_{mnva} + \text{c.c.} \,, \\
Z_{wv}^{(i)} &= \sum_{amn} \rho^{*}_{ma} z_{mn} \widetilde{\rho}_{wnva} + \text{c.c.} \,, \\
Z_{wv}^{(j)} &= -\sum_{abm} \rho^{*}_{mb} z_{ab} \widetilde{\rho}_{wmva} + \text{c.c.} \,, \\
Z_{wv}^{(k)} &= -\sum_{abm} \rho^{*}_{va} z_{bm} \widetilde{\rho}_{wmab} + \text{c.c.} \,, \\
Z_{wv}^{(l)} &= -\sum_{abm} \rho^{*}_{ma} z_{bv} \widetilde{\rho}_{wmba} + \text{c.c.} \,, \\
Z_{wv}^{(m)} &= \sum_{amn} \widetilde{\rho}^{\,*}_{mnwa} z_{mv} \rho_{na} + \text{c.c.} \,, \\
Z_{wv}^{(n)} &= -\sum_{abmn} \rho^{*}_{nmwb} z_{ab} \widetilde{\rho}_{nmva} \,, \\
Z_{wv}^{(o)} &= \sum_{abcm} \widetilde{\rho}^{\,*}_{vmbc} z_{ac} \widetilde{\rho}_{wmba} \,, \\
Z_{wv}^{(p)} &= \sum_{amnr} \widetilde{\rho}^{\,*}_{rnwa} z_{rm} \widetilde{\rho}_{mnva} \,, \\
Z_{wv}^{(q)} &= -\sum_{abmn} \rho^{*}_{vmba} z_{mn} \widetilde{\rho}_{nwab} \,, \\
Z_{wv}^{(r)} &= \sum_{abmn} \widetilde{\rho}^{\,*}_{mvaw} z_{bn} \widetilde{\rho}_{mnab} + \text{c.c.} \,, \\
Z_{wv}^{(s)} &= -\sum_{abmn} \rho^{*}_{nmwa} z_{bv} \widetilde{\rho}_{mnab} + \text{c.c.} \,, \\
Z_{wv}^{(t)} &= -\sum_{abmn} \rho^{*}_{mnba} z_{mv} \widetilde{\rho}_{nwab} + \text{c.c.}
\end{aligned}$$

The valence normalization for state v is given by

$$\begin{aligned}
(\delta N_v)_{\rm conn} = {} & \sum_{m} \rho^{*}_{mv} \rho_{mv} - \sum_{a} \rho^{*}_{va} \rho_{va} \\
& + \sum_{abm} \rho^{*}_{vmab} \widetilde{\rho}_{mvab} + \sum_{mna} \rho^{*}_{mnva} \widetilde{\rho}_{mnva} \\
& + \sum_{ma} (\widetilde{\rho}_{vmva} \rho^{*}_{ma} + \widetilde{\rho}^{\,*}_{vmva} \rho_{ma}) \,,
\end{aligned} \tag{22}$$

and is depicted in Fig. 3. In presenting results, we give the lowest-order result z_{wv} and the correction

$$Z_{\rm pair} = M_{wv} - z_{wv} \,. \tag{23}$$

The formalism for matrix elements presented here is complete through third-order MBPT, as may be verified by iterating the all-order equations algebraically, substituting into the matrix element formula, and comparing with a complete list of MBPT terms through third order.[13] In Ref. 13, following earlier work by Dzuba *et al.*,[14] we divided the third-order matrix element into structural radiation (SR) terms, and terms associated with the random phase approximation, Brueckner orbitals (BO), and normalization. Unfortunately, it is very hard to make a similar division in presenting results of

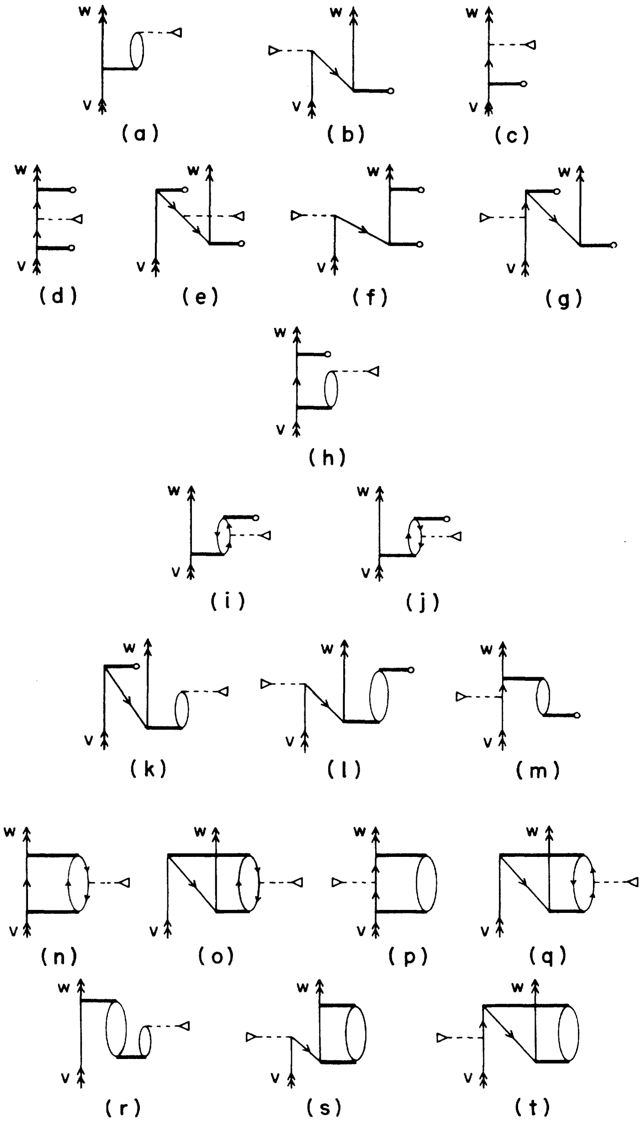

FIG. 2. The 20 Brueckner-Goldstone graphs representing all-orders corrections to matrix elements corresponding to Eq. (21). Notation is the same as in Fig. 1, and again exchange graphs are not shown.

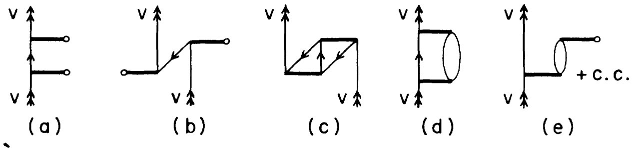

FIG. 3. Brueckner-Goldstone graphs contributing to the valence normalization factor given in Eq. (22). Graph (a) corresponds to first term in Eq. (22), etc.

our all-order formalism, because the various contributions are mixed together and are difficult to separate. For example, the diagram in Fig. 2(a) leads to both RPA and SR contributions as the equations are iterated. Even the normalization terms, as defined in Ref. 13, are not uniquely associated with the denominator in Eq. (19); the normalization terms presented in Ref. 13, in fact, result from subtle cancellations between the denominator in Eq. (19) and the BO-like diagram of Fig. 2(t). We shall, therefore, not attempt to make any detailed breakdown of the matrix element when presenting results.

One important point is that RPA terms are not fully incorporated into the present approximation. While RPA terms are complete through third order, certain fourth- and higher-order RPA terms are absent. The missing diagrams are of a type in which the "bubbles" characteristic of RPA graphs are directed both upwards and downwards, as shown in Fig. 4, where we give an example of a fourth-order RPA term which is omitted, and an example of a fourth-order RPA term which is included. It is possible to devise all-order schemes in which the full RPA approximation is included, but we shall not pursue these at the present stage, because there is empirical evidence that we have already included the most important RPA terms, as we shall discuss in Sec. IV. Furthermore, it is in a sense consistent to omit the fourth-order RPA terms that we do omit, because these would arise from the inclusion of coupled-cluster terms in the wave function; in particular, powers of S_2. Such terms, however, have been neglected throughout in the present approximation.

This completes our presentation of formulas. However, before the expressions are suitable for coding into a computer program, it is necessary to perform a rather lengthy angular momentum analysis, and to cast the formulas into the form of radial factors multiplied by angular coefficients. The appropriate all-order radial equations for one-valence-electron systems may be obtained from those for closed-shell systems given in Ref. 5. The full radial form for the matrix element, however, is too lengthy to include in the present article. To derive the expression for the matrix element, we developed a program written in the symbolic manipulation language REDUCE (Ref. 15), which embodies the standard graphical analysis rules[9] of angular momentum. The results of this program were checked by a hand evaluation. In Table IV we give a term-by-term breakdown of the hyperfine constant A of the $2s_{1/2}$ state in Li and of the $2s_{1/2}$-$2p_{1/2}$ reduced dipole matrix element in Li. This breakdown can be used for detailed comparison with other calculations.

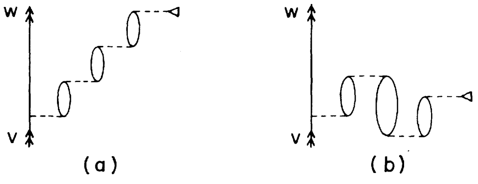

FIG. 4. (a) Fourth-order RPA graph included in the present formalism. (b) Fourth-order RPA graph not included in the present formalism. This particular graph arises from inclusion of the term $\frac{1}{2}S_2^2$ in $|\psi_V\rangle$.

Owing to the complexity of the formalism, we developed independently at least two computer codes to calculate all of the properties discussed in this paper. These codes were carefully tested against one another to reduce the possibility of coding errors.

III. PRESENTATION OF RESULTS

A. Energies

The numerical method employed to solve the all-order equations has been described in detail in Ref. 5. We use a basis set consisting of 30 positive-energy states formed from quartic splines; summation over the last five states could be eliminated with no loss of numerical significance. Details on the construction of this basis set can be found in Ref. 17. Although the basis set enables us to perform sums in one (radial) dimension with high accuracy, there remains an infinite summation over the angular momenta of the intermediate excited states; a suitable scheme must be found to extrapolate this partial-wave summation to infinity. In our work on ionization energies, we have used two different extrapolation schemes; we shall describe both, starting with the more accurate and more computationally demanding scheme.

At a given stage of calculation, the orbital angular momenta of all excited states are restricted to be less than or equal to some $L_{\max}$; other angular momenta in the problem, such as the multipolarities of terms in the partial-wave expansion of Coulomb matrix elements, are allowed to take all values consistent with triangular conditions. This restriction gives a finite number of pair coefficients to be determined iteratively. A converged solution is obtained for each value of $L_{\max}=2$, 3, 4, 5, and 6, requiring in all five, separate calculations. We present values for the Li core energy δE_C and the $2s$ valence energy δE_v in Table I for each value of $L_{\max}$. Noting the approximate $1/L_{\max}^4$ dependence of the differences $\delta E_C(L_{\max})-\delta E_C(L_{\max}-1)$, and similarly with δE_v, we fit these differences to a polynomial in $1/L_{\max}$ of the form

$$\delta E_C(L_{\max})-\delta E_C(L_{\max}-1)=\frac{A_1}{L_{\max}^4}+\frac{A_2}{L_{\max}^5}+\cdots+\frac{A_n}{L_{\max}^{n+3}} . \tag{24}$$

After such a fit, it is straightforward to sum the series for $L_{\max}>6$. In Table I we show the results from two three-

TABLE I. Accurate L extrapolation of Li 2s energy and Li$^+$ core energy.

$L_{\max}$	$2s_{1/2}$	Li$^+$ core[a]
2	−0.001 806 48	−0.042 394 6
3	−0.001 835 32	−0.043 106 3
4	−0.001 844 37	−0.043 364 2
5	−0.001 848 07	−0.043 478 9
6	−0.001 849 85	−0.043 537 1
Extrapolated		
(3-4-5)	−0.001 852 60	−0.043 636 1
(4-5-6)	−0.001 852 62	−0.043 635 1
(3-4-5-6)	−0.001 852 62	−0.043 634 7
Final	−0.001 852 6(4)	−0.043 635 (4)

[a] Core energy excludes energy-shift contribution and is not exact.

[b] Error in final result includes estimate of basis-set error.

point fits, based on $L_{\max}=3$, 4, and 5 and $L_{\max}=4$, 5, and 6, and on one four-point fit with $L_{\max}=3$, 4, 5, and 6. The results show the high stability of this extrapolation scheme. Indeed, the error in the final result is dominated by basis-set truncation error, which we have estimated from an evaluation of second-order energies with basis sets of size 30, 60, and 70.

The results for the 2s valence energy have been transferred from Table I to our general summary in Table II. For the remaining states in Table II, we have adopted a cruder partial-wave extrapolation which requires less computation. The all-order equations are solved for $L_{\max}=6$ only, and a partial-wave decomposition is made for δE_v,

$$\delta E_v=\sum_{K=0}^{K_{\max}}\delta E_v(K)\ . \tag{25}$$

The values of $K_{\max}$ are related to those of $L_{\max}$; for s states, there is a sufficient number of pair coefficients to permit evaluation up to $K_{\max}=L_{\max}$, while for p states one can evaluate up to $K_{\max}=L_{\max}-1$. One can extrapolate the partial-wave expansion (25) using a polynomial fit as described above. However, it should be noted that the extrapolation is in principle incorrect; in all of the cases that we have tested, it overestimates the true limit. The error in the extrapolation is caused by the slight $L_{\max}$ dependence of each term in the partial-wave expansion (25). For example, one finds that the $K=2$ term becomes progressively smaller in magnitude as $L_{\max}$ is increased from 2 to 6. Performing the extrapolation just described gives a result −0.001 853 4 a.u., to be compared to the more nearly correct result −0.001 825 6 a.u., from Table I. One can regard this extrapolation method as giving a lower limit to the valence energy; an upper limit is provided by the truncated $L_{\max}=6$ result from Table I, −0.001 849 9 a.u. One can now take the average of these two values and assign an error which spans the entire range from lower to upper limit; for the 2s energy this would yield −0.001 852(2) a.u.

We have adopted this extrapolation approach for all states considered in the present work apart from the Li 2s state. The dominant error is now due to the partial-wave extrapolation, and is about five times the expected basis-set truncation error. However, the overall numerical error is still small enough, in the sense that the discrepancy from experiment is somewhat larger. The principal error in the whole calculation is, therefore, the missing correlation corrections.

We turn now to a discussion of the $2p_{3/2}$-$2p_{1/2}$ fine structure, which we can in principle obtain by direct subtraction of the $2p_{3/2}$ and $2p_{1/2}$ ionization energies. Our results are summarized in Table III. It is evident that many digits are lost in making the subtraction. However, we have tested the numerical significance of the various differences and find a high degree of stability, showing

TABLE II. Summary of energies for valence states of Li and Be$^+$.

Term	$2s_{1/2}$	$2p_{1/2}$	$2p_{3/2}$	$3s_{1/2}$
			Li	
Hf	−0.196 320 4	−0.128 638	−0.128 636	−0.073 801 0
E(pair)	−0.001 852 6(4)	−0.001 606(2)	−0.001 606(2)	−0.000 389 0(4)
E(3) extra	0.000 010 6(1)	0.000 010	0.000 010	0.000 001 7
Breit	0.000 003 2	0.000 002	0.000 001	0.000 000 7
Nuclear recoil	0.000 016 2	0.000 007	0.000 007	0.000 006 0
Total	−0.198 142 9(5)	−0.130 226(2)	−0.130 225(2)	−0.074 181 6(4)
Experiment[a]	−0.198 142 2(1)	−0.130 236(0)	−0.130 235(0)	−0.074 182 0(1)
			Be$^+$	
HF	−0.666 183	−0.519 447	−0.519 406	−0.266 523 4
E(pair)	−0.003 140(3)	−0.004 364(6)	−0.004 360(6)	−0.000 733 6(8)
E(3) extra	0.000 011	0.000 018	0.000 018	0.000 001 6
Breit	0.000 018	0.000 022	0.000 008	0.000 004 4
Nuclear recoil	0.000 042	0.000 016	0.000 016	0.000 016 7
Total	−0.669 252(3)	−0.523 754(6)	−0.523 724(6)	−0.267 234 4(8)
Experiment[a]	−0.669 242(1)	−0.523 764(1)	−0.523 734(1)	−0.267 231 3(5)

[a] C. E. Moore, *Atomic Energy Levels*, Natl. Bur. Stand. Ref. Data Ser., Natl. Bur. Stand. (U.S.) Circ. No. 35 (U.S. GPO, Washington, D.C., 1971), Vol. I.

TABLE III. Fine structure of the $2p$ levels in Li and Be$^+$.

Term	$2p_{1/2}$	$2p_{3/2}$	$2p_{3/2}-2p_{1/2}$
		Li	
		($c=1.800$ fm, $t=2.3$ fm)	
HF	$-0.128\,638\,491$	$-0.128\,635\,940$	$0.000\,002\,551$
$E(2;n=70)$	$-0.001\,375\,340(60)$	$-0.001\,374\,890(60)$	$0.000\,000\,446(1)$
$E(\text{pair};L\leq 6;n=30)$	$-0.001\,604\,309(250)$	$-0.001\,603\,789(250)$	$0.000\,000\,521(25)$
$E(2;L\leq 6;n=30)$	$-0.001\,371\,693(250)$	$-0.001\,371\,227(250)$	$0.000\,000\,466(25)$
$E(3+;\text{pair};n=30)$[a]			$0.000\,000\,055(3)$
Breit	$0.000\,002\,149(2)$	$0.000\,000\,653$	$-0.000\,001\,496(2)$
Nuclear recoil	$0.000\,006\,840$	$0.000\,006\,840$	$0.000\,000\,000$
Total 1[b]			$0.000\,001\,501(3)$
Total 2[c]			$0.000\,001\,556(5)$
Experiment[d]			$0.000\,001\,534(2)$
		Be$^+$	
		($c=2.067$ fm, $t=2.3$ fm)	
HF	$-0.519\,446\,721$	$-0.519\,406\,115$	$0.000\,040\,605$
$E(2;n=70)$	$-0.003\,964\,220(80)$	$-0.003\,960\,770(80)$	$0.000\,003\,436(3)$
$E(\text{pair};L\leq 6;n=30)$	$-0.004\,357\,088(600)$	$-0.004\,353\,365(600)$	$0.000\,003\,723(130)$
$E(2;L\leq 6;n=30)$	$-0.003\,952\,244(600)$	$-0.003\,948\,755(600)$	$0.000\,003\,489(130)$
$E(3+,\text{pair};n=30)$[a]			$0.000\,000\,234(12)$
Breit	$0.000\,021\,875(14)$	$0.000\,007\,610(5)$	$-0.000\,014\,265(16)$
Nuclear recoil	$0.000\,016\,269$	$0.000\,016\,266$	$-0.000\,000\,003$
Total 1[b]			$0.000\,029\,773(17)$
Total 2[c]			$0.000\,030\,007(25)$
Experiment[e]			$0.000\,029\,980(25)$

[a] $E(3+,\text{pair};n=30)=E(\text{pair};L\leq 6;n=30)-E(2;L\leq 6;n=30)$.

[b] Total 1 equals HF$+E(2;n=70)$plus Breit+nuclear recoil.

[c] Total 2 equals $E(3+,\text{pair};n=30)$ plus total 1.

[d] C. E. Moore, *Atomic Energy Levels,* Natl. Bur. Stand. Ref. Data Ser., Natl. Bur. Stand. (U.S.) Circ. No. 35 (U.S. GPO, Washington, D.C., 1971), Vol. I.

[e] L. Johansson, Ark. Fys. **20**, 489 (1961).

that much of the basis-set truncation error is systematic between the $2p_{3/2}$ and $2p_{1/2}$ calculations and cancels on performing the subtraction. For example, for Li, we have evaluated the second-order valence energies with a basis set consisting of 70 positive energy states, and with one consisting of 60. In both cases the difference of $2p_{3/2}$ and $2p_{1/2}$ second-order energies (truncated at $L_{\max}=6$) is 466 $n$hartree. With a basis set consisting of 30 positive energy states, however, this difference becomes 466 $n$hartree, indicating a truncation error of about 5% with this reduced basis set.

The contribution to fine structure of the Coulomb correlation energy beyond second order may be estimated by subtracting the second-order energy from the converged all-order correlation energy; each calculation is performed with the same basis set (of size 30) and $L_{\max}=6$. The details of this subtraction are given in Table III. We assume a basis-set truncation error in this higher-order correlation correction of 5%, that is, the same percentage error that we found in the second-order contribution when evaluated with a basis set of size 30. Finally, we add contributions from the Breit interaction and nuclear recoil, the latter in fact being negligible. These two contributions were evaluated as described in Sec. II, using a basis set with 70 positive energy states.

B. Matrix elements

We next present our results for hyperfine constants A and B, and for reduced dipole matrix elements. The hyperfine constants A and B have their usual definitions;[16] because the electric quadrupole moment Q of ^{7}Li or ^{9}Be is not accurately known, we present values for B/Q for each element. In our hyperfine calculations, we take account of the reduced mass effect at the end of the calculation by multiplying all contributions by $[m_e/(m_e+M_{\text{nuc}})]^3$. The lowest-order radiative correction to the electron magnetic moment is also included in our hyperfine calculations. These multiplicative corrections make slight, but significant, differences for $2s$ and $3s$ hyperfine A constants. For $E1$ transition matrix elements we use two forms for the dipole operator, the length form D_L, and the velocity form D_V,

$$\mathbf{D}_L=-\sum_{i=1}^{N}\mathbf{r}_i\ , \tag{26a}$$

$$\mathbf{D}_V=i\frac{c}{\omega}\sum_{i=1}^{N}\boldsymbol{\alpha}_i\ , \tag{26b}$$

where ω is positive and equals the transition energy; in our calculations we use the experimental value of the transition energy for ω.

In Table IV we give a diagram-by-diagram breakdown of the $2s$ hyperfine constant A for Li, and of the length form of the $2s$-$2p_{1/2}$ reduced dipole matrix element in Li. The terms correspond to the 20 diagrams in Fig. 2 and Eq. (21); in addition there is a normalization contribution defined by

$$Z_{\text{norm}} = (Z_1)_{\text{conn}} \times \left[\frac{1}{\{[1+(\delta N_w)_{\text{conn}}][1+(\delta N_v)_{\text{conn}}]\}^{1/2}} - 1 \right] , \tag{27}$$

which gives the additional effect of including the normalization denominator in Eq. (19). We also give a diagram-by-diagram breakdown of the valence normalization for the $2s$ state of Li, as defined in Eq. (22) and Fig. 3. For each quantity, we give the result with fully iterated and with lowest-order coefficients. The lowest-order pair coefficients are given by

$$\rho_{mnav} = \frac{g_{mnav}}{\varepsilon_a + \varepsilon_v - \varepsilon_m - \varepsilon_n} , \tag{28}$$

and the lowest-order singles coefficients result from substituting (28) into the right-hand side of the singles equation (9a) and (9c) with $\rho_{ma} = 0$. A comparison of lowest order with iterated results enables one to judge the importance of iterating certain classes of correction to high order.

In Table V we give our results for the theoretical hyperfine constants of $2s$, $2p$, and $3s$ states in Li and Be$^+$. In Table VI, our values for the quadrupole hyperfine constant B of the $2p_{3/2}$ states in Li and Be$^+$ are presented. Reduced matrix elements for $E1$ transitions between $2s$ and $2p$ states and between $2p$ and $3s$ states in Li and Be$^+$ are presented in Table VII. The calculations presented in Tables V–VII were all performed with $L_{\max} = 6$; the effect of the partial-wave extrapolation being negligible. The dominant source of numerical error arises from the finite basis set and was estimated by evaluating Z_{pair} in lowest order (as defined above) with basis sets of various size.

IV. DISCUSSION OF RESULTS

A. Energies

It may be seen from Table II that the general level of error in valence removal energies is 10 μhartree, or

TABLE IV. Contributions to matrix elements in Li. $x[y] = x \times 10^y$.

	$A(2s_{1/2};\text{MHz})$		$\langle 2p_{1/2} \Vert ez \Vert 2s_{1/2} \rangle$	
Figure	Lowest order	Iterated	Lowest order	Iterated
2(a)	70.33(1)	95.52(2)	−0.011 60	−0.014 28
2(b)	2.7[−2]	0.70	−1.1[−6]	−2.7[−5]
2(c)	12.13	13.52	−0.029 20(1)	−0.032 86(1)
2(d)	0.13	0.16	0.000 47	0.000 61
2(e)	6.3[−7]	4.3[−4]	0	0
2(f)	−2.7[−3]	5.1[−3]	1.1[−7]	−2.0[−7]
2(g)	3.3[−5]	8.5[−4]	−4.2[−10]	−6.0[−8]
2(h)	2.11	1.50	−0.000 10	−0.000 13
2(i)	8.6[−2]	0.12	3.3[−6]	−3.8[−6]
2(j)	−2.1[−2]	2.6[−4]	0	0
2(k)	1.8[−3]	5.7[−2]	1.1[−8]	3.3[−7]
2(l)	1.2[−2]	5.1[−3]	−4.5[−7]	−2.0[−7]
2(m)	−1.7[−2]	−6.6[−3]	−4.1[−7]	2.6[−6]
2(n)	1.66	2.70	0	0
2(o)	0	0	0	0
2(p)	0.19(4)	0.28(4)	0.000 57	0.000 77
2(q)	1.30	1.87	−1.2[−5]	−1.5[−5]
2(r)	2.91	4.75	0.000 19	0.000 26
2(s)	−0.82	−1.18	3.2[−5]	4.6[−5]
2(t)	−1.43	−1.97	−8.3[−5]	−0.000 12
Normal	−0.14	−0.22	−0.001 49	−0.002 09
Total	88.44(5)	117.82(5)	−0.041 21(1)	−0.047 84(1)
	$2s$ valence normalization			
3(a)	7.81[−5]	9.62[−5]		
3(b)	−5.33[−11]	−3.62[−8]		
3(c)	−7.14[−5]	−9.99[−5]		
3(d)	3.76[−4]	5.37[−4]		
3(e)	−7.06[−7]	7.95[−7]		

TABLE V. Magnetic dipole hyperfine constants, A (Mhz), for $2s$, $2p$, and $3s$ states of Li and Be$^+$. Conversion factor: 1 a.u. $=6.579\,684\times10^9$ MHz.

Term	$2s_{1/2}$	$2p_{1/2}$	$2p_{3/2}$	$3s_{1/2}$
		^{7}Li		
	$I=3/2$ $g_I=2.170\,949(1)$	$M=7.014\,36$ a.m.u.	$m_r^3/m_e^3=0.999\,765\,4$	
HF	284.65	32.32	6.46	66.95
Pair	117.83(5)	13.63(1)	−9.49	26.29(2)
Total	402.47(5)	45.96(1)	−3.03	93.24(2)
Experiment	401.75[a]	46.17(35)[b]	−3.07(13)[c]	
		^{9}Be$^+$		
	$I=3/2$ $g_I=-0.784\,955(2)$	$M=9.009\,99$ a.m.u.	$m_r^3/m_e^3=0.999\,817\,4$	
HF	−498.23	−93.37	−18.66	−128.06
Pair	−127.40(9)	−24.57(1)	17.62(1)	−30.92(2)
Total	−625.63(9)	−117.94(1)	−1.04(1)	−158.98(2)
Experiment	−625.01[d]	−118.6(3.6)[e]	$\lvert A\rvert<0.6$[f]	

[a] R. G. Schlecht, D. W. McColm, Phys. Rev. **142**, 11 (1966).

[b] G. J. Ritter, Can. J. Phys. **43**, 770 (1965).

[c] J. D. Lyons and R. K. Nesbet, Phys. Rev. Lett. **24**, 433 (1970).

[d] D. J. Wineland, J. J. Bollinger, and W. M. Itano, Phys. Rev. Lett. **50**, 628 (1983).

[e] J. J. Bollinger, J. S. Wells, D. J. Wineland, and W. M. Itano, Phys. Rev. A **31**, 2711 (1985).

[f] O. Poulsen, T. Anderson, and N. Skouboe, J. Phys. B **8**, 1393 (1975).

0.01%. Two exceptions are the $2s$ and $3s$ valence energies in Li. As we shall discuss shortly, the extra accuracy here is probably fortuitous. The treatment of the Breit interaction and nuclear recoil should be accurate to about 1 μhartree or less, and so the principal source of error is presumably the omitted fourth-order effects, namely the coupled-cluster terms and the fourth-order triples. We can partially verify this conclusion by making use of the coupled-electron pair approximation (CEPA) scheme CEPA-1 described by Ahlrichs[18] to estimate the order of magnitude of coupled-cluster terms. This scheme involves modifying the energy factors on the left-hand sides of (9a)–(9d) by adding certain energy shifts. We find a contribution of order $+10$ μhartree for $2p_{1/2}$. Alternatively, we can infer the size of coupled-cluster terms by subtracting our pair-correlation energy from that calculated by Lindgren,[1] who included the dominant coupled-cluster terms in his iterative procedure. This suggests a contribution of size $+22$ μhartree for the $2p_{1/2}$ state. We expect the remaining discrepancy to be primarily due to the omitted fourth-order triples, suggesting that these contributions also enter at the 10-μhartree level for the $2p_{1/2}$ state. As for the $2s$ state, we estimate coupled-cluster terms to be $+10$ μ hartree from use of the CEPA-1 scheme, and infer them to be $+19$ μhartree from comparison with the calculation of Lindgren. The discrepancy with experiment in the present calculation, however, is on the order of 1 μ hartree, implying that there is a high degree of cancellation between the coupled-cluster contributions and the fourth-order triples for the $2s$ state. Interestingly, this cancellation does not seem to persist for the same state in the next member of the isoelectronic series, Be$^+$.

TABLE VI. Electric quadrupole hyperfine constants, B/Q (MHz/b), for $2p_{3/2}$ states. Conversion factor: 1 a.u. $=234.9647$ MHz/b.

Term	Li $2p_{3/2}$	Be$^+$ $2p_{3/2}$
HF	5.492	43.86
Pair	−0.159(3)	−0.67(5)
Total	5.333(3)	43.19(5)
Other	5.325(1)[a] 5.363[c]	41[b]

[a] I. Lindgren, Ref. 1.

[b] J. L. Heully and A.-M. Mårtensson-Pendrill, Phys. Scr. **31**, 169 (1985).

[c] R. K. Nesbet, Phys. Rev. A **2**, 661 (1970).

We believe that the next level of accuracy, the 1-μhartree level, can be reached by including both the fourth-order triples and the fourth-order coupled-cluster terms in the calculation. While it is in principle possible to do this within the framework of an all-order approach, the computer memory required to store the triple excitation coefficients ρ_{mnrabc} in a reasonably complete calculation would be prohibitively large, especially in a fully relativistic formulation. An alternative scheme is to identify the omitted terms from fourth-order MBPT, and to evaluate them individually, in much the same way that we have done with $E^{(3)}_{\text{extra}}$ in the present work. Because the MBPT terms can be coded essentially as nested loops, there is relatively little demand on computer memory.

Turning now to the fine-structure results in Table III, we find agreement with experiment at the 20-$n$hartree level for both Li and Be$^+$. As we shall see, the relatively close agreement with experiment for Be$^+$ is probably fortuitous. Some of the discrepancy is due to our incomplete treatment of the Coulomb correlation. From a consideration of the size of the omitted fourth-order effects in the $2p_{1/2}$ and $2p_{3/2}$ ionization energies, we expect the omitted Coulomb correlation for the fine structure to be on the order of 1% of the second-order correction, that

TABLE VII. Reduced matrix elements for $E1$ transitions between $2s$ and $2p$ states and between $2p$ and $3s$ states in Li and Be$^+$. L and V refer to length and velocity forms [Eqs. (26a) and (26b)], respectively.

Term	L	V	L	V	L	V	L	V
				Li				
	$2s_{1/2}$-$2p_{1/2}$		$2s_{1/2}$-$2p_{3/2}$		$2p_{1/2}$-$3s_{1/2}$		$2p_{3/2}$-$3s_{1/2}$	
	$\omega=0.067\,906\,07$		$\omega=0.067\,907\,62$		$\omega=0.056\,054\,13$		$\omega=0.056\,052\,58$	
HF	3.364	3.419	−4.758	−4.835	2.487	2.470	3.518	3.494
Pair	−0.048	−0.101	0.068	0.143	−0.055	−0.038	−0.077	−0.054
Total	3.316	3.317	−4.690	−4.692	2.433	2.433	3.441	3.440
Expt.	3.305(1)[a]		−4.674(2)[a]		2.48(11)[b]		3.51(15)[b]	
				Be$^+$				
	$2s_{1/2}$-$2p_{1/2}$		$2s_{1/2}$-$2p_{3/2}$		$2p_{1/2}$-$3s_{1/2}$		$2p_{3/2}$-$3s_{1/2}$	
	$\omega=0.145\,478$		$\omega=0.145\,508$		$\omega=0.256\,533$		$\omega=0.256\,503$	
HF	1.874	1.965	−2.651	−2.780	0.882	0.890	1.248	1.258
Pair	−0.024	−0.114	0.034	0.162	−0.014	−0.022	−0.020	−0.031
Total	1.850	1.851	−2.617	−2.618	0.868	0.868	1.227	1.227
Expt.[c]	1.80(2)		−2.54(3)		0.89(6)		1.26(8)	

[a] A. Gaupp, P. Kuske, and H. J. Andrä, Phys. Rev. A **26**, 3351 (1982).

[b] G. A. Martin and W. L. Wiese, J. Phys. Chem. Ref. Data **5**, 537 (1976).

[c] J. Bromander, Phys. Scr. **4**, 61 (1971).

is, about 5 $n$hartree for Li, and about 40 $n$hartree for Be$^+$. However, a substantial amount of error must also arise from our incomplete treatment of correlation corrections to the Breit interaction. This seems likely in view of the fact that the highest-order terms that we have included in the Breit correlation, the third-order BO terms (defined in Ref. 9), are -119 $n$hartree for the Li fine structure and -545 $n$hartree for the Be$^+$ fine structure. It would perhaps be interesting to incorporate the Breit interaction into the iterative procedure to attempt to refine the calculation of the fine-structural interval. We note in passing that radiative corrections to the fine structure are about 5 $n$hartree for Li and about 70 $n$hartree for Be$^+$.

B. Matrix elements

In general, a critical comparison of our matrix elements with experiment is hampered by the relatively large experimental errors. An exception to this statement is provided by the $2s$ hyperfine constant, which is known experimentally with high precision. We shall, therefore, discuss the hyperfine constant first and in detail.

Referring to the $2s$ hyperfine entry in Table IV, we see that the dominant diagrams are Figs. 2(a) and 2(r), which correspond mainly to the important RPA effects, and Fig. 2(c), which corresponds to BO effects. Smaller contributions come from Figs. 2(b), 2(s), and 2(t), which correspond mainly to BO effects, and from Figs. 2(n) and 2(q), which are predominantly SR contributions. There are very small, but just significant, contributions from Fig. 2(d), a BO cross term, from Fig. 2(h), a BO modification to an RPA effect, and from the normalization. In general, diagrams which involve core singles coefficients ρ_{ma} are very small or completely negligible. The suppression of core singles relative to valence singles may be understood on energy denominator grounds: the energy required to excite a $1s$ electron to a $2s$ state is 2.60 hartree, while the corresponding energy for excitation of a $2s$ valence electron to a $3s$ state is only 0.12 hartree.

In order to put the all-order calculation of hyperfine structure in perspective, we have summarized in Table VIII the result of our present calculation together with results of our earlier calculations employing MBPT at various levels. We see that RPA effects are very important, accounting for about 90% of the correlation. The second-order correction, which is the leading RPA effect, is large, but there are substantial contributions from higher-order RPA terms. The next most important term is the third-order BO term. In general, the sum of all-order RPA corrections and third-order BO corrections forms an accurate approximation for the whole series of alkali-metal atoms from Li to Cs, as shown by our earlier work in Ref. 2. For Li, the level of accuracy achieved within this approximation is about 0.5%, and this rises to about 3% in the heavier alkali-metal atoms, where the BO contributions are relatively more important. We next consider the effect of the additional third-order diagrams besides the RPA and BO contributions already discussed; these are the SR and normalization terms for which explicit formulas are given in Ref. 13. These enter at the right level to account for the remaining correlation, but have the wrong sign. We have found a similar situation for matrix elements in Na, showing that at least fourth-order MBPT corrections are required in order to produce a significant improvement in accuracy beyond the results given in Ref. 2. The present method leads to a significant improvement over the results of third-order MBPT. From Table IV, we see that to improve upon the results of Ref. 2, one needs to add the third-order SR terms, and in addition fourth-order terms in which an RPA effect is modified by a BO effect [Fig. 2(h)], and fourth-order BO terms [from the difference between the iterated Fig. 2(c) and the lowest-order Fig. 2(c)]. Other effects are general-

TABLE VIII. Contributions to the Li $2s_{1/2}$ hyperfine constant, A (MHz), in various approximations.

Approximation	Value	Δ% (from experiment)
$Z(1)$	284.65	−29.15
$Z(1)+Z(2)$	354.96(1)	−11.65
$Z(1)+Z(\mathrm{RPA})$	390.29(1)	−2.85
$Z(1)+Z(\mathrm{RPA})+Z(3;\mathrm{BO})$	400.30(1)	−0.36
$Z(1)+Z(\mathrm{RPA})+Z(3;\mathrm{extra})$[a]	399.19(1)	−0.64
$Z(1)+Z(\mathrm{pair})$	402.47(5)	0.18
Experiment	401.75	

[a] $Z(3;\mathrm{extra})$ indicates the sum of all third-order contributions besides the third-order RPA already included in $Z(\mathrm{RPA})$.

ly at the level of the present discrepancy with experiment.

As mentioned above, our all-order formulation of the matrix element does not incorporate fully the RPA. We would expect the $2s$ hyperfine structure to be quite sensitive to omission of important parts of the RPA sequence, as RPA effects constitute the majority of the correlation. Since our final result is in such close agreement with experiment, however, we conclude that the dominant RPA terms are already included in the present approach. Nevertheless, it may be interesting to consider schemes in which the RPA is fully included, as it is possible that the omitted RPA trems form a substantial part of the remaining correlation.

Moving on to the hyperfine constants for the other states, we note that our theoretical results for $2p_{1/2}$ hyperfine parameters (Table V) are probably rather more accurate than the experimental values, with which they agree. The hyperfine A factors for the $2p_{3/2}$ states are interesting because there is a high degree of cancellation between the HF value and the higher-order correlation, notably the RPA contribution. Our previous result for Li from third-order MBPT was −3.71 MHz,[2] in significant disagreement with experiment. In the present all-order approach, however, we obtain −3.03 MHz, in agreement with experiment. As for the electric quadrupole constants (Table VI), the theoretical error is probably at about the same level as the numerical error indicated in the table, and we find good agreement with the calculation of Lindgren,[1] which includes a slightly different set of terms. As noted by Lindgren, it is not possible to use these values for B/Q to improve the accuracy of our knowledge of Q, as the experimental uncertainties in B are too high.

Finally, we consider our results for $E1$ transition matrix elements given in Table VII. The level of disagreement between the length and velocity results is small, on the order of 0.05%, and we tentatively take this as an indication of the level of theoretical error in the calculation. As higher-order correlation effects are added, we expect the length and velocity calculations to come into closer agreement. The $2p$-$3s$ matrix elements are in agreement with experiment, and are probably somewhat more accurate than the experimental values. However, there is a clear disagreement between theory and experiment for the $2s$-$2p$ matrix elements; in every case, the experimental value is smaller in magnitude than our prediction. Similar discrepancies have been found by other authors: our value 3.317 a.u. for the $2s$-$2p_{1/2}$ matrix element in Li is in excellent agreement with the value 3.318 a.u. obtained by Sims *et al.*[19] using a method based on Hylleraas coordinates, and with the value 3.319 a.u. obtained by Froese-Fischer[20] using a multiconfiguration HF code. The precise cause of these discrepancies with experiment is not fully understood at present, but in view of the close agreement between different theoretical approaches, it seems likely that the problem lies on the experimental side.

In summary, we have presented the results of a numerically accurate, fully relativistic implementation of the basic pair approximation in Li and Be^+. The approximation gives valence removal energies accurate to about 0.01% (or 10 μhartree), and matrix elements accurate to 0.2% or less. The principal error in the calculation arises from omitted correlation effects, which enter in fourth order for both valence removal energies and matrix elements. We believe that the accuracy of these calculations could be improved, perhaps to the 1-μhartree level for removal energies, by including these omitted fourth-order effects perturbatively. However, the next stage in our calculations is to apply the present treatment to heavier one-valence-electron atoms, notably Rb, Cs, and Tl, which are of great interest on account of the need to interpret measurements of parity-nonconserving and time-reversal violating effects. Here a fully relativistic many-body treatment such as we have given in essential. We expect the level of accuracy for these heavy atoms to be somewhat worse than for three-electron atoms, where MBPT converges relatively quickly. In Cs, for example, third-order MBPT gives hyperfine parameters and allowed $E1$ transition matrix elements accurate at the 3–5 % level, while one is already obtaining accuracies of order 0.5% at this level with three-electron systems.[2] Our hope is that the present technique, or a slight modification of it, will yield hyperfine parameters and $E1$ matrix elements accurate to the 1% level (or less) in these heavy atoms. If this is so, then the technique could be extended to the parity-nonconserving and time-reversal violating problems with great profit.

ACKNOWLEDGMENTS

We would like to thank Ingvar Lindgren, Anne-Marie Pendrill, Yong-Ki Kim, and George Victor for discussions. This work was partially supported by National Science Foundation (NSF) Grant No. PHY86-08101. Some of the work was carried out at the Institute for Theoretical Physics, University of California, Santa Barbara, which is supported by NSF Grant No. PHY82-17853, supplemented by funds from NASA. Much of the numerical work was carried out on the Cray XMP/48 at the National Center for Supercomputing Applications, which is supported by NSF Grant No. PHY88-0007N.

APPENDIX

In this appendix we shall prove Eq. (19). It is sufficient to show

$$\langle \psi_w | Z | \psi_v \rangle = \delta_{wv} (Z_0)_{\rm conn} \langle \psi_v | \psi_v \rangle + (Z_1)_{\rm conn} N_0 \ , \tag{A1}$$

$$\delta N_v = (\delta N_v)_{\rm conn} N_0 \ , \tag{A2}$$

where the core normalization N_0 is defined by (18).

As a preliminary, we shall outline briefly a proof of the following well-known result for a diagonal matrix element in a closed-shell system,

$$\langle \psi | Z | \psi \rangle = \langle \psi | \psi \rangle \langle \psi | Z | \psi \rangle_{\rm conn} \ . \tag{A3}$$

We shall assume the result of Lindgren and Morrison,[9]

$$|\psi\rangle = \{\exp(S)\} |0_C\rangle \ , \tag{A4}$$

where S is a purely connected operator, and $|0_C>$ is the closed-shell core in the zeroth-order approximation. Thus, expanding the exponential,

$$\langle \psi | Z | \psi \rangle = \sum_{n=0}^{\infty} \sum_{m=0}^{\infty} \frac{1}{n!m!} \langle 0_C | \{ (S^\dagger)^m \} Z \{ S^n \} | 0_C \rangle \ . \tag{A5}$$

Now, the crux of the proof is the following "partitioning" identity:[12]

$$\begin{aligned} &\langle 0_C | \{ (S^\dagger)^m \} Z \{ S^n \} | 0_C \rangle \\ &\quad = \sum_{n'=0}^{n} \sum_{m'=0}^{m} \frac{m!n!}{m'!n'!(m-m')!(n-n')!} \\ &\qquad \times \langle 0_C | \{ (S^\dagger)^{m'} \} Z \{ S^{n'} \} | 0_C \rangle_{\rm conn} \\ &\qquad \times \langle 0_C | \{ (S^\dagger)^{m-m'} \} \{ S^{n-n'} \} | 0_C \rangle \ . \end{aligned} \tag{A6}$$

This equation may be understood by considering Wick's theorem expansion of the left-hand side. Each term in this expansion must have the form of a connected part involving Z, multiplied by a residual factor containing the uncontracted operators $S^\dagger$ and S. By Wick's theorem, this residual factor must be proportional to

$$\langle 0_C | \{ (S^\dagger)^{m-m'} \} \{ S^{n-n'} \} | 0_C \rangle \ . \tag{A7}$$

The numerical factor in Eq. (A6) is a weighting factor giving the number of ways in which m' objects can be selected from m, and n' objects from n. One may now insert Eq. (A6) into Eq. (A5), and resum the exponentials by means of

$$\sum_{n=0}^{\infty} \sum_{n'=0}^{n} \to \sum_{n'=0}^{\infty} \sum_{\nu=0}^{\infty} , \quad \nu = n - n' \ . \tag{A8}$$

This yields the required result (A3).

We shall now extend this proof to situations involving one-valence-electron systems. Here the exact wave function is given by

$$|\psi_v\rangle = \Omega_v a_v^\dagger |0_C\rangle = \{\exp(S_v)\} a_v^\dagger |0_C\rangle \ , \tag{A9}$$

where v denotes the valence electron, S_v is purely connected, and $|0_C\rangle$ is again the closed-shell core. Let us consider the numerator first:

$$\langle \psi_w | Z | \psi_v \rangle = \sum_{n=0}^{\infty} \sum_{m=0}^{\infty} \frac{1}{n!m!} \langle 0_C | a_w \{ (S_w^\dagger)^m \} Z \{ S_v^n \} a_v^\dagger | 0_C \rangle \tag{A10}$$

We again factor the terms in Wick's theorem expansion of the right-hand side into connected parts involving Z, and a residue. This time, however, there are two categories of connected part, according to whether a_w and a_v are or are not included with Z (a_w and a_v must go together, otherwise there would be an odd number of annihilation and creation operators and the expression would vanish). The generalization of (A6) is thus

$$\begin{aligned} &\langle 0_C | a_w \{ (S_w^\dagger)^m \} Z \{ S_v^n \} a_v^\dagger | 0_C \rangle \\ &\quad = \sum_{m'=0}^{n} \sum_{n'=0}^{n} \frac{m!n!}{m'!n'!(m-m')!(n-n')!} \\ &\qquad \times (\langle 0_C | \{ (S_w^\dagger)^{m'} \} Z \{ S_v^{n'} \} | 0_C \rangle_{\rm conn} \langle 0_C | a_w \{ (S_w^\dagger)^{m-m'} \} \{ S_v^{n-n'} \} a_v^\dagger | 0_C \rangle \\ &\qquad + \langle 0_C | \overline{a_w [\{ (S_w^\dagger)^{m'} \} Z \{ S_v^{n'} \}] a_v^\dagger} | 0_c \rangle_{\rm conn} \langle 0_C | \{ (S_w^\dagger)^{m-m'} \} \{ S_v^{n-n'} \} | 0_C \rangle) \ . \end{aligned} \tag{A11}$$

The bar notation used here is explained below Eq. (17). Using this expression and resumming exponentials as before gives

$$\begin{aligned}\langle \psi_w | Z | \psi_v \rangle = {} & \langle 0_C | \Omega_w^\dagger Z \Omega_v | 0_C \rangle_{\text{conn}} \langle 0_C | a_w \Omega_w^\dagger \Omega_v a_v^\dagger | 0_C \rangle \\ & + \langle 0_C | \overline{a_w (\Omega_w^\dagger Z \Omega_v) a_v^\dagger} | 0_C \rangle_{\text{conn}} \\ & \times \langle 0_C | \Omega_w^\dagger \Omega_v | 0_C \rangle \; . \end{aligned} \tag{A12}$$

The first term contains the overlap $\langle \psi_w | \psi_v \rangle = \delta_{wv} \langle \psi_v | \psi_v \rangle$, while the second involves $\langle 0_C | \Omega_w^\dagger \Omega_v | 0_C \rangle = N_0$ (the parts of Ω_w and Ω_v depending upon the valence states do not contribute). Thus finally we obtain the desired identity Eq. (A1).

Similarly one has

$$\begin{aligned}\delta N_v & = \langle 0_C | \overline{a_v (\Omega_v^\dagger \Omega_v) a_v^\dagger} | 0_C \rangle \\ & = \langle 0_C | \overline{a_v (\Omega_v^\dagger \Omega_v) a_v^\dagger} | 0_C \rangle_{\text{conn}} \langle 0_C | \Omega_v^\dagger \Omega_v | 0_C \rangle \\ & = (\delta N_v)_{\text{conn}} N_0 \; . \end{aligned} \tag{A13}$$

where the second line follows from the usual sort of partitioning argument.

This completes the proof of Eq. (19). Note that this proof applies to any operator Z, whether of one-body, two-body, etc., type.

---

[1] I. Lindgren, Phys. Rev. A **31**, 1273 (1985).

[2] W. R. Johnson, M. Idrees, and J. Sapirstein, Phys. Rev. A **35**, 3218 (1987).

[3] W. R. Johnson, S. A. Blundell, and J. Sapirstein, Phys. Rev. A **37**, 2764 (1988).

[4] F. W. King and V. Shoup, Phys. Rev. A **33**, 2940 (1986); F. W. King, *ibid.* **38**, 6017 (1988).

[5] S. A. Blundell, W. R. Johnson, Z. W. Liu, and J. Sapirstein, Phys. Rev. A **39**, 3768 (1989).

[6] A. Weiss, Phys. Rev. **132**, 1826 (1961); Astrophys. J. **138**, 1262 (1963); B. F. Davis and K. T. Chung, Phys. Rev. A **29**, 2586 (1984).

[7] I. Lindgren (private communication).

[8] F. Coester and H. Kümmel, Nucl. Phys. **17**, 477 (1960).

[9] I. Lindgren and J. Morrison, *Atomic Many-Body Theory,* 2nd ed. (Springer-Verlag, Berlin, 1986).

[10] W. R. Johnson, S. A. Blundell, and J. Sapirstein, Phys. Rev. A **38**, 2699 (1988).

[11] D. S. Hughes and Carl Eckart, Phys. Rev. **36**, 694 (1930).

[12] A. L. Fetter and J. D. Walecka, *Quantum Theory of Many-Particle Systems* (McGraw-Hill, New York, 1971).

[13] S. A. Blundell, D. S. Guo, W. R. Johnson, and J. Sapirstein, At. Data Nucl. Data Tables **37**, 1103 (1987).

[14] V. A. Dzuba, V. V. Flambaum, P. G. Silvestrov, and O. P. Sushkov, J. Phys. B **20**, 3297 (1987).

[15] A. C. Hearn, Stanford University Report No. ITP-247 (unpublished).

[16] H. Kopfermann, *Nuclear Moments* (Academic, New York, 1958).

[17] W. R. Johnson, S. A. Blundell, and J. Sapirstein, Phys. Rev. A **37**, 307 (1988).

[18] R. Alrichs, Comput. Phys. Commun. **17**, 31 (1979).

[19] J. S. Sims, S. A. Hagstrom, and J. R. Rumble, Phys. Rev. A **13**, 242 (1976).

[20] Charlotte Froese-Fischer, Nucl. Instrum. Methods Phys. Res. B **31**, 265 (1988).